Boosting the Oxygen Evolution Reaction via the Reconstruction of $M(OH)_x/Fe_3O_4$ Catalyst

Xiaoqu Wang,[a,c,†] Limin Wang,[a,†] Yongchun Liu,[a,†] Rajkumar Devasenathipathy,[b] Li Liu,[a] Qiulan Huang,[a] Dujuan Huang,[a] Youjun Fan,*[a] Du-Hong Chen*[a] and Wei Chen*[a]

[a] *Guangxi Key Laboratory of Low Carbon Energy Materials, School of Chemistry and Pharmaceutical Sciences, Guangxi Normal University, Guilin 541004, China*

[b.] *Institute of Advanced Materials (IAM), Nanjing Tech University (Nanjing Tech), Nanjing 211816, China*

[c.] *School of Materials and Energy, Institute of Energy Storage Technologies, Yunnan University, Kunming 650091, China*

* Corresponding authors.

E-mail addresses: youjunfan@mailbox.gxnu.edu.cn (Y. Fan), dhchen@gxnu.edu.cn (D. H. Chen), weichen@mailbox.gxnu.edu.cn (W. Chen).

† These authors contributed equally to the work.

1. Supporting Theoretical Calculation Details

The Vienna Ab initio Simulation Package was used for all density functional theory (DFT) calculations.[1] Utilizing the PBE generalized gradient approximation exchange-correlation function, the projector augmented wave pseudopotential was employed in the computations.[2,3] To account for strongly localized d-electrons for Ni and Fe, all metal oxide energetics were computed using the DFT with the Hubbard-U framework (DFT+U). According to linear response theory, the Hubbard-U correction terms were at U_{eff}(Ni) = 6.2 eV and U_{eff}(Fe) = 5.3 eV. The adsorption energy was calculated using K-sampling with a Monkhorst-Pack mesh of 3×3×1, the DOS was calculated using 9 × 9 × 1, and the cutoff energy of the plane waves basis set was 500 eV. The ultimate force on each atom was less than 0.05 eV $Å^{-1}$, all structures were spin polarized, and all atoms were totally relaxed with an energy convergence tolerance of 10^{-5} eV per atom.

The adsorption energy of intermediates was computed using the following Equation (1):

$$\Delta G_{ads} = E_{ads} - E_{*} + \Delta E_{ZPE} - T\Delta S \qquad (1)$$

Where ads represents OH*, O*, OOH*, and the ($E_{ads} - E_{*}$) corresponds to the binding energy, ΔE_{ZPE} refers to the zero-point energy change, ΔS was regarded as the entropy change. The calculated ΔE_{ZPE} and ΔS were grasped by vibration frequency calculation.

The Gibbs free energy of the four reaction steps refers to the following four Equations (2) – (5):

$$* + O_2 + e^- + H_2O = *OOH + OH^- \qquad (2)$$

$$*OOH + e^- = *O + OH^- \qquad (3)$$

$$*O + e^- + H_2O = *OH + OH^- \qquad (4)$$

$$*OH + e^- = * + OH^- \qquad (5)$$

2. Supporting Figures and Table

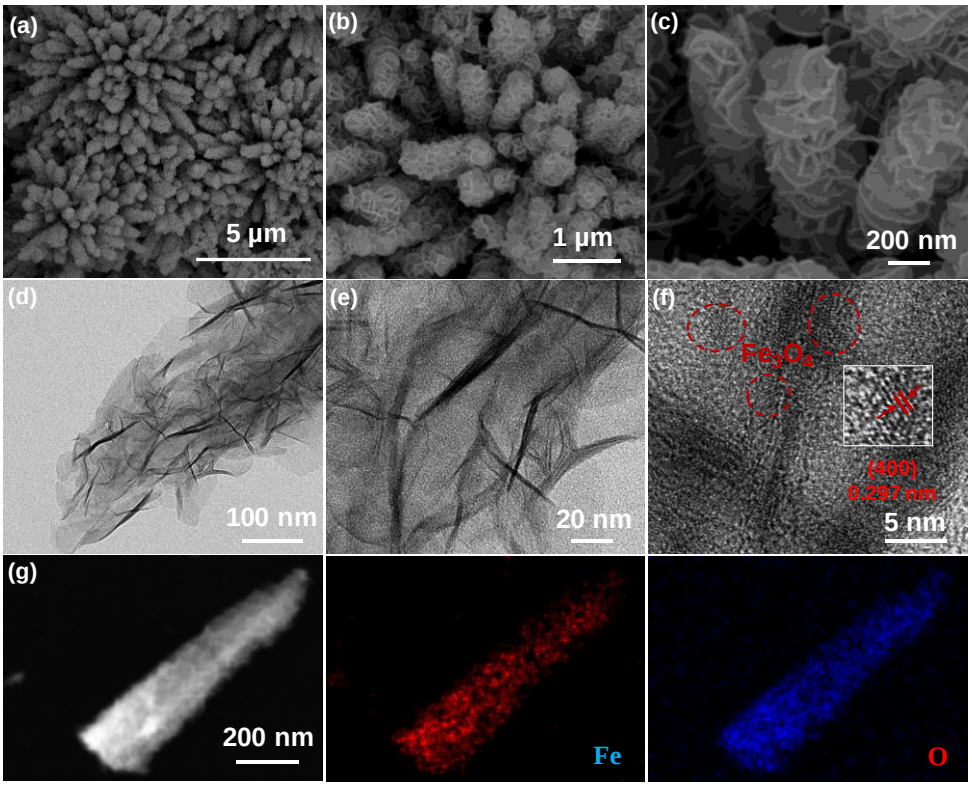

Fig. S1 SEM (a–c) and TEM (d–g) images Fe_3O_4/IF.

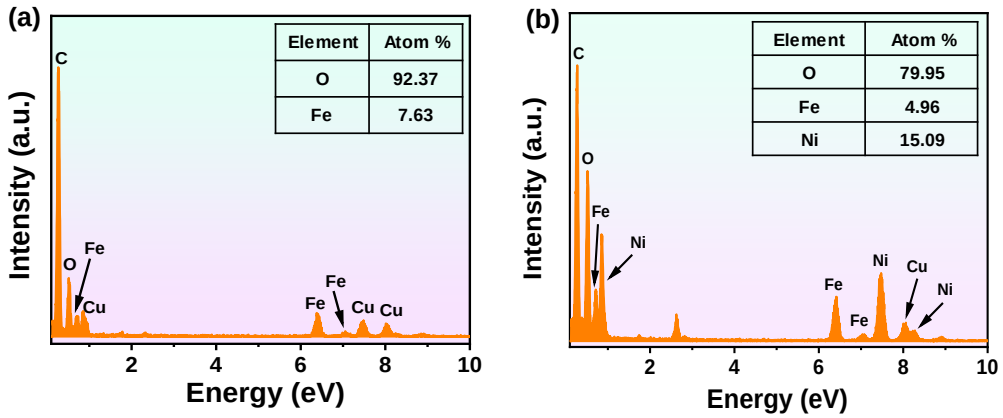

Fig. S2 TEM-EDX spectra of Fe_3O_4/IF (a) and $M(OH)_x/Fe_3O_4$/IF (b).

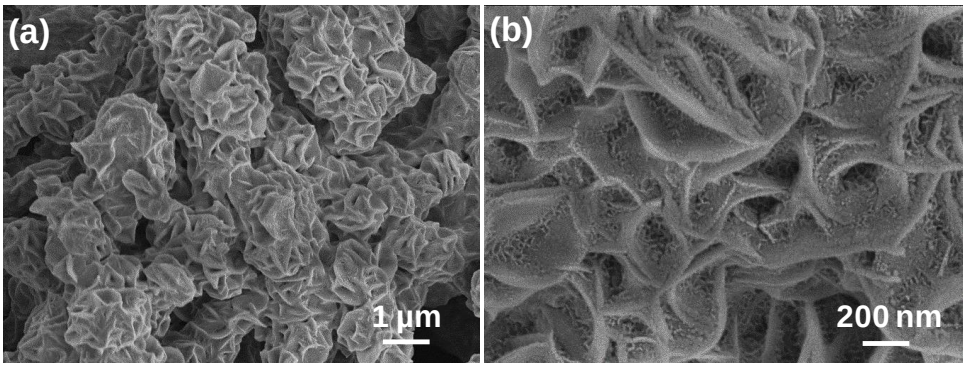

Fig. S3 SEM images of $M(OH)_x/Fe_3O_4$/IF (H_2O).

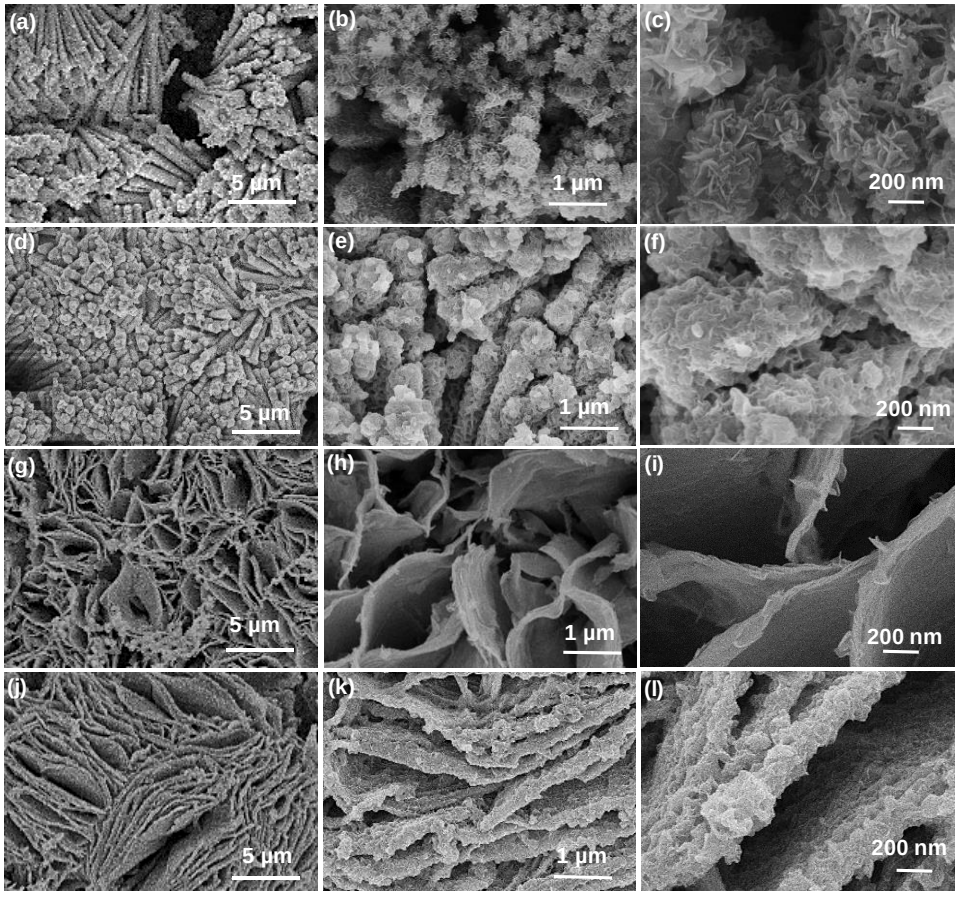

Fig. S4 (a–c) SEM images of Fe_3O_4/IF (SO_4^{2-}). (d–f) SEM images of $M(OH)x/Fe_3O_4$/IF (SO_4^{2-}). (g–i) SEM images of Fe_3O_4/IF (Br^-). (j–l) SEM images of $M(OH)_x/Fe_3O_4$/IF (Br^-).

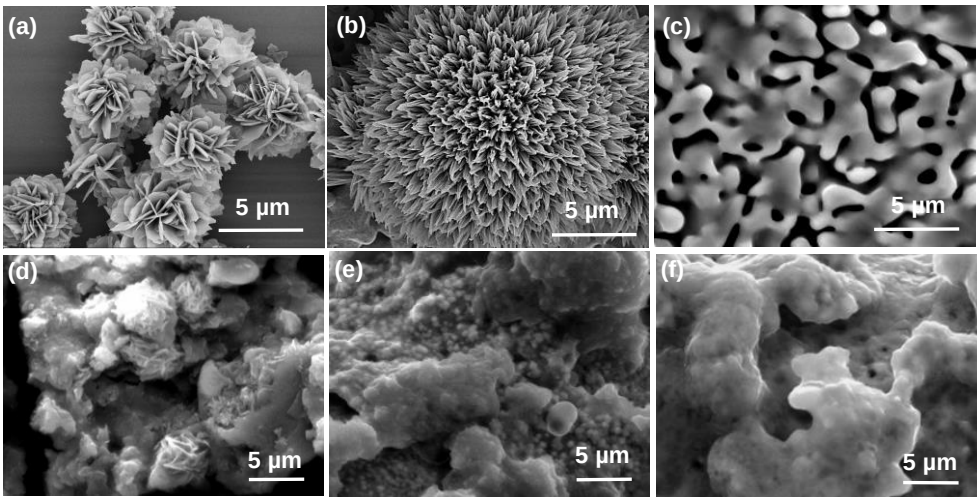

Fig. S5 SEM images of Fe_3O_4 powder (a), Fe_3O_4/IF (no metal salts) (b), IF (c), $M(OH)_x/Fe_3O_4$ powder (d), $M(OH)_x/Fe_3O_4$/IF (no metal salts) (e), and $M(OH)_x$/IF (f).

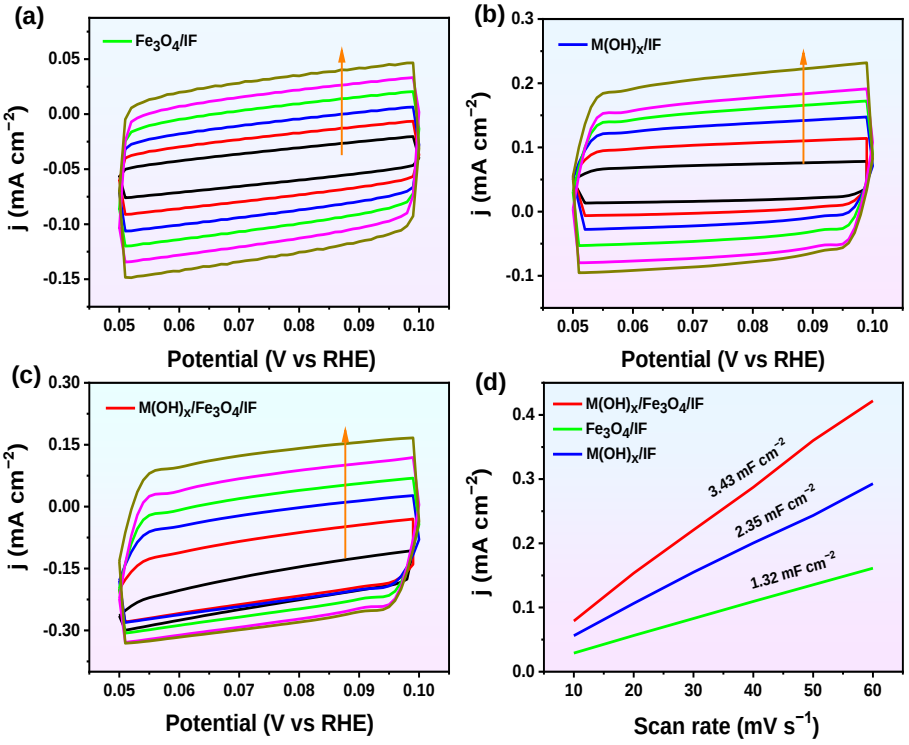

Fig. S6 Cyclic voltammograms of Fe_3O_4/IF (a), $M(OH)_x$/IF (b), and $M(OH)_x/Fe_3O_4$/IF (c) recorded at a double layer region with the increasing scan rates of 10, 20, 30, 40, 50, and 60 mV s^{-1}. (d) The plots of current density vs scanning rate.

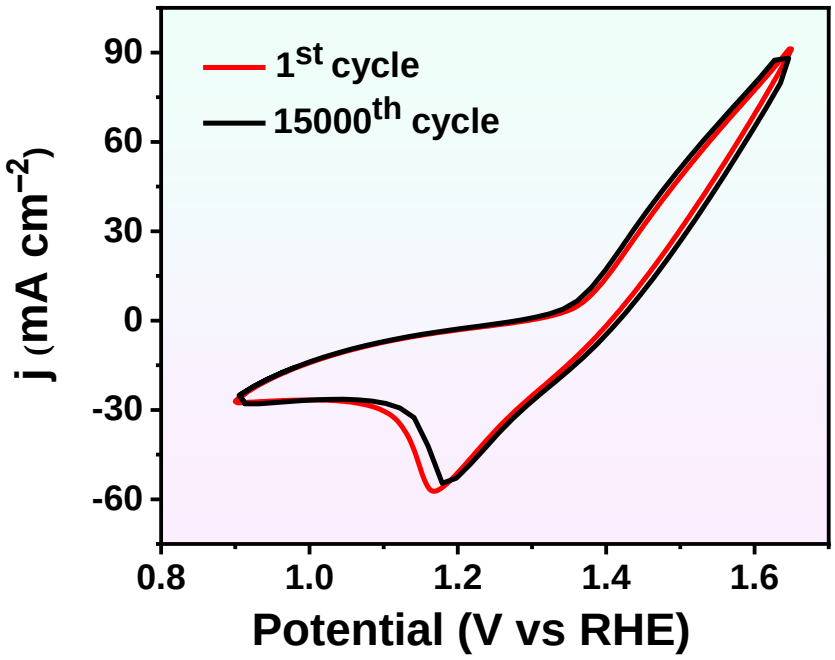

Fig. S7 The CV curves of the 1 st and 15000 th of $M(OH)_x/Fe_3O_4$/IF electrode at the potential of 0.9 to 1.65 V vs. RHE recorded in N_2-saturated 1 M KOH at 100 mV s^{-1}.

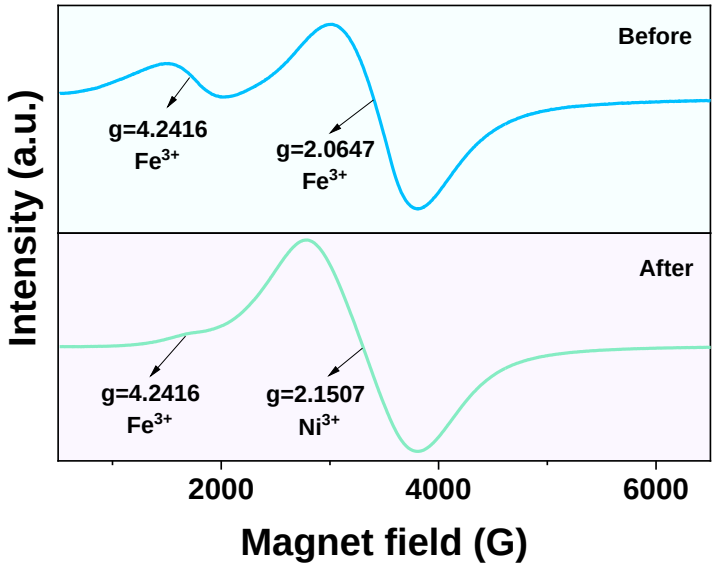

Fig. S8 The EPR spectra of $M(OH)_x/Fe_3O_4$/IF electrode before and after OER measurement.

Table S1. Comparisons of catalytic performance of $M(OH)_x/Fe_3O_4$/IF and other electrocatalysts reported recently for OER.

Catalyst	Electrolyte	Overpotentials (mV)@ Currrent density ($mA\ cm^{-2}$)	Tafel slope (mV dec^{-1})	Stability (h)	Ref.
$M(OH)_x/Fe_3O_4$/IF	**1 M KOH**	**214@50 311@500**	**57**	**70**	**This work**
2% Ru-NCO	1 M KOH	233@50 269@100	59	25	*Chem. Eng. J.* **2022**, *439*, 135634.
NCF-C3	1 M KOH	343@100	63	20	*Chem. Eng. J.* **2021**, *426*, 130785.
B-MOF-Zn-Co	1 M KOH	362@100	66.8	300	*Small* **2023**, 2308517.
Ni-B-P micro spheres	1 M KOH	360@300	153	120	*Chem. Eng. J.* **2023**, *462*, 142177.
Ni_3S_2/NF	1 M KOH	330@100	70	2.8	*Adv. Mater.* **2017**, *29*, 1701584.
VOx/Ni_3S_2@NF	1 M KOH	330@100			*J. Mater. Chem. A* **2019**, *7*, 10534-10542.
NiSO-2	1 M KOH	320@100 400@500	46	100	*Chem. Eng. J.* **2023**, *475*, 146140.
CoP-Co_2P@PC/PG NHs	1 M KOH	272@20	66		*Small* **2019**, *15*, 1804546.
NiFeB hydroxide nanosheets	1 M KOH	252@100		130	*Nat. Commun.* **2022**, *13*, 6094.

Supporting References

1. G. K. J. Furthmiiller, Efficient Iterative Schemes for ab Initio Total-Energy Calculations Using a Plane-Wave Basis Set, *Phys. Rev. B* 1996, **54**, 11169.
2. P. E. Blöchl, Projector Augmented-Wave Method, *Phys. Rev. B*, 1994, **50**, 17953–17979.
3. K. B. John P. Perdew, Matthias Ernzerhof, Generalized Gradient Approximation Made Simple, *Phys. Rev. Lett.*, 1996, **77**, 3865.